

The role of Coulomb interaction in superconducting NbTiN thin films

D. Hazra¹, N. Tsavdaris², A. Mukhtarova¹, M. Jacquemin², F. Blanchet¹, R. Albert¹, S. Jebari¹, A. Grimm¹, E. Blanquet², F. Mercier², C. Chapelier¹ and M. Hofheinz¹

¹ *Univ. Grenoble Alpes, CEA, INAC-Pheliqs, 38000 Grenoble, France and*

² *Univ. Grenoble Alpes, CNRS, Grenoble INP, SIMaP, 38000 Grenoble, France**

(Dated: November 15, 2017)

We report on the superconducting properties of Nb_{1-x}Ti_xN thin films of thickness ~ 10 nm, with different Ti fraction x in the range $0 \leq x \leq 0.5$, deposited by high temperature chemical vapor deposition. In this parameter range, we observe that the superconducting critical temperature (T_c) increases with x . Our analysis, in accordance with both McMillan's and Finkelstein's theories, shows that disorder-enhanced Coulomb interaction decreases with x , leading to an increase of T_c .

Keywords: NbTiN, superconductivity, disordered superconductor, Coulomb interaction, chemical vapor deposition

Because of its high superconducting critical temperature, high-quality NbTiN has been one of the most preferred materials for many superconducting applications, such as superconducting coating for radio frequency cavities [1–3]. The high superconducting energy gap (Δ) makes NbTiN very suitable for THz application, such as superconductor-insulator-superconductor mixtures and bolometers [4–7]. NbTiN is also a preferred material for optical single photon detection [8–11] and has been used as high characteristic impedance microwave resonator [12]— thanks to its very high kinetic inductance. Low loss resonators can be fabricated from NbTiN [13, 14]; this in combination with high Δ , T_c , and B_{c2} make NbTiN a potential alternative to aluminum for circuit quantum electrodynamics in high magnetic field [12].

The effect of disorder on conventional s-wave superconductivity has been extensively studied in Nb_{1-x}Ti_xN and its parent compounds, NbN and TiN [15–27]. Already vast and rich physics has been unearthed in these systems, that include superconductor-insulator transition [15, 17], observation of a pseudogap regime above T_c [20, 21], disorder-induced phase fluctuation [21], spatially inhomogeneous superconductivity [19, 26, 27] and enhancement of pair breaking parameter [23].

Despite numerous applications and fundamental investigations the following points are clearly missing: (1) A controlled growth technique to deposit high quality thin films. (2) A clear understanding of the variation of superconducting parameters with Ti fraction (x). (3) A systematic way to control electronic disorder and to study its effect on superconducting properties. Here, we report on the superconducting properties of high-quality Nb_{1-x}Ti_xN films where electronic disorder can be tuned by controlling x . The T_c of our samples increases with x which we attribute to the reduction of Coulomb interaction. This is consistent with both McMillan's and Finkelstein's equations.

To grow Nb_{1-x}Ti_xN thin films, d.c. magnetron sputtering is the most common technique [12, 14, 28–32], but atomic layer deposition (ALD) has also been explored [33]. In the case of sputtering, the high sputtering rate makes the thickness control very challenging below 10 nm; whereas, in case of ALD, the control of both composition and crystalline quality remains difficult.

Variations of superconducting parameters, especially T_c , with Ti fraction x , have been previously reported [34]. The authors observed that T_c remains almost constant up to $x \sim 0.5$ and decreases for higher values. In contrast, Myoren et al. [35] observed a monotonous decrease of T_c with x for three of their films with $x = 0, 0.34$ and 0.62 , respectively. In both cases, the films constituted 3d systems with thicknesses above 300 nm and were prepared by dc magnetron sputtering. Prior to these experiments, Pressal et al. [36] and Yen et al. [37] observed that T_c varies non-monotonically with x ; below $x \sim 0.4$, T_c increases with x and decreases above. In either of these cases, no clear explanation for the observed variation of T_c with Ti fraction was provided.

To study the effect of disorder on superconducting properties, majority of the experiments have been focussed on series of films with different thicknesses, making it difficult to disentangle bulk disorder to surface scattering contributions.

Here, to overcome these issues, we report on the superconducting properties of five Nb_{1-x}Ti_xN thin films of thickness 10 nm grown by high temperature chemical vapor deposition (HTCVD). The detailed structural analysis by x-ray diffraction and cross sectional high resolution transmission electron microscopy reveal that the deposited films are of very high crystalline qualities. Apart from different gas flow rates, chamber conditions are kept identical between each depositions. In this way, the only parameter changing from sample to sample is the Ti fraction (x), which we control in the range $0 \leq x \leq 0.5$ for the present study. Our goal is to understand how x , in the range $0 \leq x \leq 0.5$, impacts disorder and T_c . Disorder will be estimated with the Ioffe-Regel parameter $k_F \ell$ (k_F is the Fermi wavevector and ℓ is the mean free path).

Five Nb_{1-x}Ti_xN thin films have been produced by

* iamdibyenduhazra@gmail.com

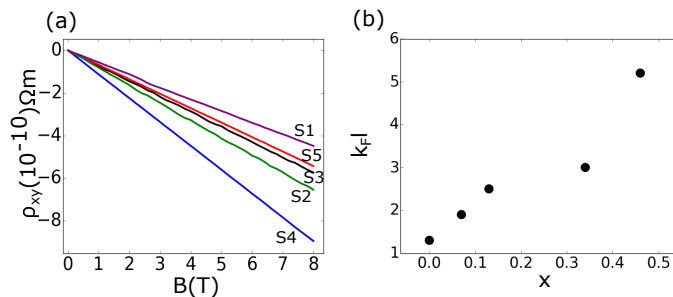


FIG. 1. (a) ρ_{xy} for all five samples at 50 K as a function of magnetic field. (b) The variation of Ioffe-Regel parameter ($k_F\ell$), determined at 50 K, as a function of Ti fraction (x).

HTCVD at 1100 °C on Epiready (0001) oriented Al_2O_3 substrate. Deposition apparatus and thermodynamics calculation have been reported elsewhere [38]. Deposition conditions are the same for each sample except for the ratio of chlorine species $\text{NbCl}_x/\text{TiCl}_x$ in the gas phase. The control of the Nb/Ti ratio in the gas phase allows the control of the titanium concentration in the layer. All the films are $d = 10 \pm 1$ nm thick, as determined from x-ray reflectometry.

The films are pure cubic NbTiN (ICDD: 01-088-2404); no hexagonal phases were detected. The XRD (111)- ω scan rocking curve values, referring to the tilt angle along the 111 direction between grains, are low and between 190 and 350 arcsec with no clear dependence on Ti fraction. Thus, the crystalline quality of NbTiN is not affected by the presence of Ti. However, two NbTiN in-plane variants with an in-plane twist relationship of 60° are detected in all samples. These in-plane variants results from the stacking of material with a cubic structure (NbTiN) on a hexagonal substrate (surface of (0001) Al_2O_3). We found that the domains with a single variant were distributed randomly and have a lateral size in the order of 150 nm [38, 39].

Electrical transport measurements were performed in a Quantum Design Physical Property Measurement System down to 2.5 K and up to magnetic field (B) 8 T. The free electron parameters of our samples were determined from the combination of longitudinal and Hall resistivity measurement at 50 K; lower temperatures are avoided not to be influenced by superconducting fluctuation related effects [40–42]. Fig. 1a shows the variation of Hall resistivity (ρ_{xy}) for all five samples as a function of magnetic field. For all five samples, ρ_{xy} varies linearly with magnetic field. The free electron density (n) is determined from the slope of the $\rho_{xy}(B)$ curve, i.e., from the Hall coefficient $R_H = 1/ne$, where e is the charge of the electron. Knowing n , k_F and v_F (the Fermi velocity) are determined from $k_F = (3\pi^2n)^{1/3}$ and $v_F = \hbar k_F/m$, where m is the mass of the electron. The elastic scattering time (τ) is estimated from Drude's formula: $\rho_{xx} = m/ne^2\tau$, here $\rho_{xx} = dR_S$ is the longitudinal resistivity at 50 K. The other important free electron parameters, like, ℓ , diffusion constant (D) and density

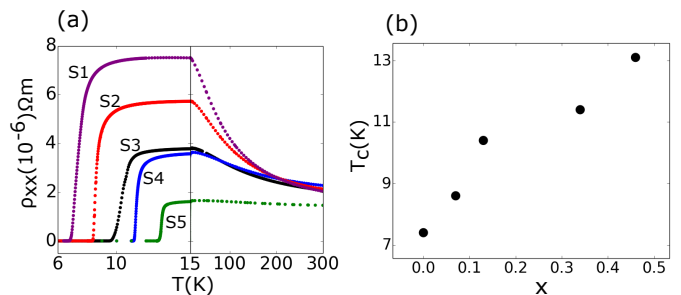


FIG. 2. (a) Temperature dependence of ρ_{xx} for all five samples down to the superconducting transition temperature. (b) The variation of T_c as a function of Ti fraction showing a monotonic dependence.

of states at the Fermi level (N_V) are determined from $\ell = v_F\tau$, $D = v_F\ell/3$ and $N_V = mk_F/\hbar^2\pi^2$. $k_F\ell$ is determined from $k_F\ell = \frac{\hbar}{e^2}\rho_{xx}^{-1}\left(\frac{9}{8}\pi eR_H\right)^{1/3}$. We note that $k_F\ell$ depends only on experimentally measured quantities R_H and ρ_{xx} , not on effective electron mass m . The important free electron parameters are summarized for each sample in Table-I.

In Fig. 1b, we plot $k_F\ell$ as a function of x , showing that $k_F\ell$ increases monotonically with x . Thus, the disorder can be tuned systematically by controlling Ti fraction, making these films ideal candidates to study the effect of atomic level disorder on superconducting properties. This observation is consistent with our structural analysis [38], where we observed that surface morphology improved with increasing Ti fraction. This is also consistent with the fact that, both residual resistivity ratio (RRR) and ℓ increases with x (see Table-I; RRR is defined as $\rho_{xx}(300\text{ K})/\rho_{xx}(\text{max})$). It is well-known that RRR decreases with increasing defect density [43] that subsequently reduces ℓ . At 50 K where free electron parameters are defined, the electron-phonon interaction is small and thus the electrical resistance stems predominantly from the electron-defect scattering [44, 45].

In Fig. 2a, we plot the temperature dependence of ρ_{xx} at zero magnetic field. Upon cooling down from room temperature ρ_{xx} increases and reaches a maximum at some intermediate temperature T_{max} . Below T_{max} , ρ_{xx} starts to decrease with decreasing temperature due to the onset of superconductivity. The left panel of Fig. 2a shows a magnified version near the superconducting transition. Clearly T_c is systematically increasing with Ti fraction from sample S1 ($x = 0$) to S5 ($x = 0.5$). This is shown in Fig. 2b where T_c is plotted as a function of x . T_c is defined at a temperature where ρ_{xx} is half of normal resistivity defined by ρ_{xx} measured at 15 K. In Table-I, we summarize T_c of our samples.

To understand the variation of T_c with x , we follow two different approaches: (1) McMillan's equation and (2) Finkelstein's equation.

The T_c of a strongly coupled superconductor like NbTiN is governed by McMillans equation [46]

TABLE I. An overview of some of the important parameters of our Nb_{1-x}Ti_xN thin films. The directly measured parameters and those extracted from the free electron theory are separated by the double-line.

Samples	a (Å)	x	RRR	T_c (K)	R_H ($10^{-11} \text{m}^3/\text{C}$)	R_S (50 K) (Ω)	n ($10^{28}/\text{m}^3$)	τ (10^{-17}s)	ℓ (Å)	$k_F \ell$ (50 K)	D ($10^{-5} \text{m}^2/\text{s}$)	N_V ($\frac{10^{47} \text{states}}{\text{m}^3}$)
S1	4.340	0.00	0.27	7.4	5.6	607	11.1	5.2	0.9	1.3	5.1	1.24
S2	4.339	0.07	0.37	8.6	8.4	502	7.4	9.6	1.4	1.9	7.1	1.10
S3	4.336	0.14	0.55	10.4	7.9	362	7.8	12.5	1.9	2.5	9.7	1.10
S4	4.312	0.34	0.63	11.4	13.8	349	4.5	22.4	2.8	3.1	12.0	0.92
S5	4.303	0.46	0.88	13.1	6.8	167	9.2	23.0	3.7	5.2	19.8	1.17

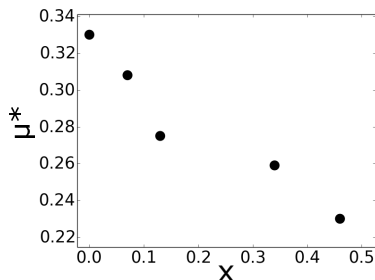


FIG. 3. Variation of the Coulomb pseudo-potential as a function of Ti fraction.

$$T_c = \frac{\Theta_D}{1.14} \exp\left(-\frac{1.04(1+\lambda)}{\lambda - \mu^*(1+0.62\lambda)}\right). \quad (1)$$

Here, Θ_D is the Debye temperature, λ is the effective electron-phonon coupling constant, and μ^* is the Coulomb pseudopotential representing electronic Coulomb repulsion. λ is given by $\lambda = N_V U$, where U is the attractive potential. Θ_D and U depend on the phonon structure and hence lattice parameter (a). μ^* , on the other hand, depends on disorder—with increasing disorder, μ^* increases [47]. Our five samples have different a , N_V , and $k_F \ell$. Therefore, Θ_D , λ , and μ^* are different for all five samples. Thus, it is difficult to analyze the variation of T_c as a function of any of the single variables— a , N_V , or $k_F \ell$. However, we note that the maximum change in a is less than 1% between our samples. Thus, the change in Θ_D from sample to sample due to change in a is not enough to describe the variation of T_c . N_V , on the other hand, changes quite significantly—the maximum variation is about 25%. However, we see no systematic variation of T_c with N_V . For instance, S1 has highest N_V but it also has lowest T_c ; on the other hand, S4 has lowest N_V but it has second highest T_c (see Table-I). In contrast, the variation of T_c with $k_F \ell$ is more systematic. The maximum variation in $k_F \ell$ is about 250%, much more than a or N_V . Thus, it seems that with increasing x , disorder of our system reduces, resulting a decrease in μ^* . This according to Eq.1, increases T_c .

To verify this mechanism, we assume that λ and Θ_D are the same for all our samples. According to Kihlstrom

et al. [48] $\lambda = 1.46$ and $\mu^* = 0.33$ for NbN (S1). Substituting this in Eq.1 yields $\Theta_D = 183 \text{K}$ for S1. Now substituting $\Theta_D = 183 \text{K}$ and $\lambda = 1.46$, we determine μ^* from Eq.1 for the remaining samples (S2 to S5). In Fig. 3, we show the variation of μ^* as a function of x . The observed decrease of μ^* with increasing Ti fraction corresponds to decreasing Coulomb interaction, in agreement with the $k_F \ell$ parameters we extracted.

Here, we would like to mention that $\Theta_D = 183 \text{K}$ is small compared to the values reported in reference [45] and references therein which range between 250 to 350 K. This is due to the fact that T_c in reference [48] was 14.0 K larger than S1. Taking $T_c = 14.0 \text{K}$ yields $\Theta_D = 346 \text{K}$. Irrespective of exact value of Θ_D , the qualitative behavior of Fig. 3 remains the same.

Using McMillan's equation, we have argued that increase of T_c with increasing x can most likely be attributed to Coulomb interaction. But, we had to assume that Θ_D and λ do not change from sample to sample. We will now explore Finkelstein's formula which allows us to express T_c in terms of experimentally measured quantities, normal sheet-resistance R_s and τ . Thus, unlike McMillan's equation, there is no free parameter in this framework.

Finkelstein's model states that with the increasing disorder the reduced scattering length reinforces the Coulomb interaction, which in turn reduces the T_c from the non-disordered value according to the following equation:

$$\frac{T_c}{T_{c0}} = e^\gamma \left(\frac{1/\gamma - \sqrt{t/2} + t/4}{1/\gamma + \sqrt{t/2} + t/4} \right)^{1/\sqrt{2t}} \quad (2)$$

Here, T_{c0} is the critical temperature for non-disordered material, $t = R_s e^2 / \pi h$, $\gamma = \ln(h/k_B T_{c0} \tau)$.

In Fig. 4a, we plot R_s , measured at 50 K where free electron parameters are defined, as a function of x . Clearly R_s decreases with x .

To apply Finkelstein's equation, in Fig. 4b, we plot T_c as a function of R_s . The solid line is a fit, taking T_{c0} and τ as fit parameters. We extract $T_{c0} = 16.1 \text{K}$ and $\tau = 5.9 \times 10^{-16} \text{s}$ from the fit. τ , as extracted from the fit, is of the same order of magnitude as estimated from the free electron theory (see Table-I). T_{c0} , on the other hand, is close to bulk T_c reported on Nb_{1-x}Ti_xN samples, which typically range between 16 to 17 K [34, 49]. However, we

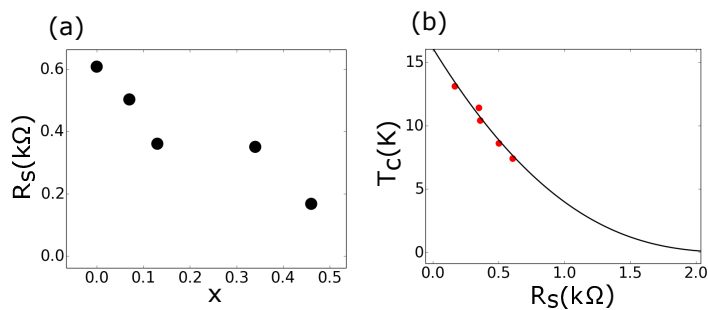


FIG. 4. (a) Variation of sheet resistance as a function of Ti fraction. (b) Variation of T_c as a function of sheet-resistance. The solid line is a fit with Finkel'stein's equation.

would like to point out that each sample, in principle, can have different T_{c0} and τ . Thus, the extracted T_{c0} and τ only represent average values.

We would like to point out that Finkelstein's model is valid for 2d systems. Our films' thickness (10 nm) is roughly twice $\xi(0)$ (see supplementary information for $\xi(0)$ measurement). Thus, our samples are not exactly in the 2d limit, but very close to it.

In summary, we report on the superconducting properties of five disordered $Nb_{1-x}Ti_xN$ thin films of thickness 10 nm with different x . We see that the disorder of the films decrease with increase of x . Consequently, with the increase of x , the disorder-induced Coulomb interaction reduces, leading to an increase of T_c . Our analysis shows quantitative agreement with the Finkelstein's theory of disordered superconductivity.

Acknowledgments— We acknowledge financial support from the French National Research Agency/grant ANR-14-CE26-0007-WASI, from the Grenoble Nanosciences Foundation/grant JoQOLaT and from the European Research Council under the European Unions Seventh Framework Programme (FP7/2007-2013)/ERC Grant agreement No 278203-WiQOJo.

-
- [1] C. Benvenuti, P. Chiggiato, L. Parrini, and R. Russo, Nuclear Instruments and Methods in Physics Research Section B: Beam Interactions with Materials and Atoms **124**, 106 (1997).
- [2] P. Fabricatore, G. Gemme, R. Musenich, R. Parodi, M. Viviani, B. Zhang, and V. Buscaglia, IEEE transactions on applied superconductivity **3**, 1761 (1993).
- [3] P. Bosland, S. Cantacuzene, J. Gobin, M. Juillard, and J. Martignac, J. Proc. of the 6th Workshop on RF Superconductivity, B. Bonin Ed, 1028 (1993).
- [4] J. Kooi, J. Stern, G. Chattopadhyay, H. LeDuc, B. Bumble, and J. Zmuidzinas, International journal of infrared and millimeter waves **19**, 373 (1998).
- [5] B. Bumble, H. LeDuc, J. Stern, and K. Megerian, IEEE transactions on applied superconductivity **11**, 76 (2001).
- [6] B. Jackson, A. Baryshev, G. De Lange, J.-R. Gao, S. Shitov, N. Iosad, and T. Klapwijk, Applied Physics Letters **79**, 436 (2001).
- [7] L. Jiang, S. Shiba, T. Shiino, K. Shimbo, N. Sakai, T. Yamakura, Y. Irimajiri, P. Ananthasubramanian, H. Maezawa, and S. Yamamoto, Superconductor Science and Technology **23**, 045025 (2010).
- [8] S. Miki, T. Yamashita, H. Terai, and Z. Wang, Optics express **21**, 10208 (2013).
- [9] C. Schuck, W. H. Pernice, and H. X. Tang, Scientific reports **3**, 1893 (2013).
- [10] M. G. Tanner, C. Natarajan, V. Pottapenjara, J. O'Connor, R. Warburton, R. Hadfield, B. Baek, S. Nam, S. Dorenbos, E. B. Ureña, *et al.*, Applied Physics Letters **96**, 221109 (2010).
- [11] S. Dorenbos, E. Reiger, U. Perinetti, V. Zwiller, T. Zijlstra, and T. Klapwijk, Applied Physics Letters **93**, 131101 (2008).
- [12] N. Samkharadze, A. Bruno, P. Scarlino, G. Zheng, D. DiVincenzo, L. DiCarlo, and L. Vandersypen, Physical Review Applied **5**, 044004 (2016).
- [13] R. Barends, N. Verduyssen, A. Endo, P. De Visser, T. Zijlstra, T. Klapwijk, P. Diener, S. Yates, and J. Baselmans, Applied Physics Letters **97**, 023508 (2010).
- [14] R. Barends, H. Hortensius, T. Zijlstra, J. J. Baselmans, S. Yates, J. Gao, and T. M. Klapwijk, IEEE Transactions on Applied Superconductivity **19**, 936 (2009).
- [15] A. Goldman and N. Markovic, Phys. Today **51**, 39 (1998).
- [16] R. Crane, N. Armitage, A. Johansson, G. Sambandamurthy, D. Shahar, and G. Grüner, Physical Review B **75**, 184530 (2007).
- [17] T. Baturina, A. Y. Mironov, V. Vinokur, M. Baklanov, and C. Strunk, Physical review letters **99**, 257003 (2007).
- [18] T. Baturina, C. Strunk, M. Baklanov, and A. Satta, Physical review letters **98**, 127003 (2007).
- [19] B. Sacépé, C. Chapelier, T. Baturina, V. Vinokur, M. Baklanov, and M. Sanquer, Physical review letters **101**, 157006 (2008).
- [20] B. Sacépé, C. Chapelier, T. I. Baturina, V. M. Vinokur, M. R. Baklanov, and M. Sanquer, Nature Communications **1**, 140 (2010).
- [21] M. Mondal, A. Kamlapure, M. Chand, G. Saraswat, S. Kumar, J. Jesudasan, L. Benfatto, V. Tripathi, and P. Raychaudhuri, Physical review letters **106**, 047001 (2011).
- [22] M. Mondal, S. Kumar, M. Chand, A. Kamlapure, G. Saraswat, G. Seibold, L. Benfatto, and P. Raychaudhuri, Physical review letters **107**, 217003 (2011).
- [23] E. Driessen, P. Coumou, R. Tromp, P. De Visser, and T. Klapwijk, Physical review letters **109**, 107003 (2012).
- [24] P. Coumou, E. Driessen, J. Bueno, C. Chapelier, and T. Klapwijk, Physical Review B **88**, 180505 (2013).
- [25] M. Mondal, A. Kamlapure, S. C. Ganguli, J. Jesudasan, V. Bagwe, L. Benfatto, and P. Raychaudhuri, Scientific Reports **3**, 1357 (2013).
- [26] A. Kamlapure, T. Das, S. C. Ganguli, J. B. Parmar, S. Bhattacharyya, and P. Raychaudhuri, Scientific reports **3**, 2979 (2013).
- [27] Y. Noat, V. Cherkez, C. Brun, T. Cren, C. Carbillat, F. Debontridder, K. Ilin, M. Siegel, A. Semenov, H.-W.

- Hübers, *et al.*, Physical Review B **88**, 014503 (2013).
- [28] H. Bell, Y. Shy, D. Anderson, and L. Toth, Journal of Applied Physics **39**, 2797 (1968).
- [29] R. Barends, H. Hortensius, T. Zijlstra, J. Baselmans, S. Yates, J. Gao, and T. Klapwijk, Applied Physics Letters **92**, 223502 (2008).
- [30] K. Makise, H. Terai, M. Takeda, Y. Uzawa, and Z. Wang, IEEE transactions on applied superconductivity **21**, 139 (2011).
- [31] T. Hong, K. Choi, K. Ik Sim, T. Ha, B. Cheol Park, H. Yamamori, and J. Hoon Kim, Journal of Applied Physics **114**, 243905 (2013).
- [32] A. Karimi, D. La Grange, N. Goebbels, and A. Santana, Thin Solid Films **607**, 14 (2016).
- [33] J. A. Klug, N. G. Becker, N. R. Groll, C. Cao, M. S. Weimer, M. J. Pellin, J. F. Zasadzinski, and T. Proslie, Applied Physics Letters **103**, 211602 (2013).
- [34] R. Di Leo, A. Nigro, G. Nobile, and R. Vaglio, Journal of Low Temperature Physics **78**, 41 (1990).
- [35] H. Myoren, T. Shimizu, T. Iizuka, and S. Takada, IEEE transactions on applied superconductivity **11**, 3828 (2001).
- [36] N. Pessall, R. Gold, and H. Johansen, Journal of Physics and Chemistry of Solids **29**, 19 (1968).
- [37] C. Yen, L. Toth, Y. Shy, D. Anderson, and L. Rosner, Journal of Applied Physics **38**, 2268 (1967).
- [38] N. Tsavdaris, D. Harza, S. Coindeau, G. Renou, F. Robaut, E. Sarigiannidou, M. Jacquemin, R. Reboud, M. Hofheinz, E. Blanquet, *et al.*, Chemistry of Materials (2017).
- [39] F. Mercier, S. Coindeau, S. Lay, A. Crisci, M. Benz, T. Encinas, R. Boichot, A. Mantoux, C. Jimenez, F. Weiss, *et al.*, Surface and Coatings Technology **260**, 126 (2014).
- [40] K. S. Tikhonov, G. Schwiete, and A. M. Finkel'stein, Physical Review B **85**, 174527 (2012).
- [41] N. P. Breznay, K. Michaeli, K. S. Tikhonov, A. M. Finkel'Stein, M. Tendulkar, and A. Kapitulnik, Physical Review B **86**, 014514 (2012).
- [42] D. Destrz, K. Ilin, M. Siegel, A. Schilling, and J. Chang, Physical Review B **95**, 224501 (2017).
- [43] C. Kittel, *Introduction to solid state physics* (Wiley, 2005).
- [44] M. Chand, A. Mishra, Y. Xiong, A. Kamlapure, S. Chockalingam, J. Jesudasan, V. Bagwe, M. Mondal, P. Adams, V. Tripathi, *et al.*, Physical Review B **80**, 134514 (2009).
- [45] M. Chand, PhD Thesis, Tata Institute of Fundamental Research, India; <http://www.tifr.res.in/superconductivity/pdfs/madhavi.pdf> (2012).
- [46] W. L. McMillan, Phys. Rev. **167**, 331 (1968).
- [47] P. W. Anderson, K. A. Muttalib, and T. V. Ramakrishnan, Phys. Rev. B **28**, 117 (1983).
- [48] K. Kihlstrom, R. Simon, and S. Wolf, Physica B+C **135**, 198 (1985).
- [49] D. Hazra, N. Tsavdaris, S. Jebari, A. Grimm, F. Blanchet, F. Mercier, E. Blanquet, C. Chapelier, and M. Hofheinz, Superconductor Science and Technology **29**, 105011 (2016).

Supplemental Material: The role of Coulomb interaction in superconducting NbTiN thin films

D. Hazra¹, N. Tsavdaris², A. Mukhtarova¹, M. Jacquemin², F. Blanchet¹, R. Albert¹,
S. Jebari¹, A. Grimm¹, E. Blanquet², F. Mercier², C. Chapelier¹ and M. Hofheinz¹
¹ *Univ. Grenoble Alpes, CEA, INAC-Phelips, 38000 Grenoble, France and*
² *Univ. Grenoble Alpes, CNRS, Grenoble INP, SIMaP, 38000 Grenoble, France**
(Dated: November 15, 2017)

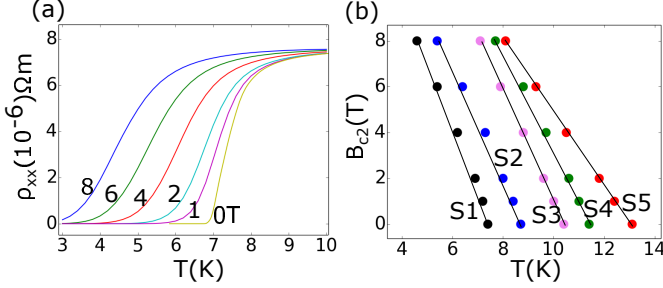


FIG. S1. (a) Temperature dependence of ρ_{xx} for S1 at different magnetic fields as indicated in the figure. (b) The variation of B_{c2} as a function of temperature for all five samples. The solid lines are straight line fits.

TABLE S1. $\left. \frac{dB_{c2}}{dT} \right|_{T=T_c}$ and $\xi(0)$ of our $\text{Nb}_{1-x}\text{Ti}_x\text{N}$ thin films.

Samples	$\left. \frac{dB_{c2}}{dT} \right _{T=T_c}$ (T/K)	$\xi(0)$ (nm)
S1	3.23	6.1
S2	2.60	5.8
S3	2.41	5.5
S4	2.30	5.3
S5	1.60	5.8

Determination of $\xi(0)$:

The zero temperature Ginzburg-Landau coherence length ($\xi(0)$) is estimated from $\xi(0) = \sqrt{\Phi_0/2\pi T_c \left. \frac{dB_{c2}}{dT} \right|_{T=T_c}}$ [1]. For that, magnetoresistance data are collected for all the samples up to a magnetic field of 8T. In Fig. S1a, we show the magnetoresistance data for S1, where temperature variation of ρ_{xx} is recorded at five different fields. $B_{c2}(T)$ is determined as the point where ρ_{xx} is half of the normal resistivity. In Fig. S1b, we plot B_{c2} as a function of temperature. The solid lines are straight line fits. The slopes and the $\xi(0)$ are listed in Table-S1.

[1] M. Tinkham, Introduction to superconductivity, Dover (1996).

* iamdibyenduhazra@gmail.com